




Fabric Analysis and Chronology at Ga-Mohana Hill North Rockshelter, Southern Kalahari Basin: Evidence for In Situ, Stratified Middle and Later Stone Age Deposits

Jayne Wilkins^{1,2,3}  · Benjamin J. Schoville^{2,3,4} · Kyle S. Brown^{2,3} · Luke Gliganic⁵ · Michael C. Meyer⁵ · Emma Loftus^{3,6} · Robyn Pickering^{3,7} · Benjamin Collins^{2,3,8} · Alexander F. Blackwood^{3,9} · Simangaliso Makalima^{2,3} · Amy Hatton^{3,10} · Sechaba Maape¹¹

Published online: 9 March 2020
© Springer Nature Switzerland AG 2020

Abstract

Over the last few decades, investigations of the southern African Late Pleistocene archeological record have transformed our understanding of *Homo sapiens* origins and evolution. However, the intensity of research on coastal and near-coastal records has surpassed that in the deep interior. One reason for the geographic bias is the rarity of well-preserved, datable rockshelter sites outside the more mountainous and karstic regions of South Africa. Here, we report stratified Middle Stone Age and Later Stone Age deposits at Ga-Mohana Hill North Rockshelter (GHN), near Kuruman, in the Northern Cape, South Africa. Contrary to a previous report, we show that the archeological deposits are in good context with minimal disturbance based on a detailed fabric analysis of plotted finds. Three dating methods, single-grain optically stimulated luminescence, radiocarbon, and uranium-thorium, indicate that the artifact-bearing deposits date to ~105 ka, ~31 ka, and ~15 ka. Thus, Ga-Mohana Hill North Rockshelter provides an important opportunity to investigate early human adaptation in this semiarid region of southern Africa.

Keywords Middle Stone Age · Later Stone Age · Fabric analysis · Kalahari · Geochronology

Electronic supplementary material The online version of this article (<https://doi.org/10.1007/s41982-020-00050-9>) contains supplementary material, which is available to authorized users.

✉ Jayne Wilkins
jayne.wilkins@griffith.edu.au

Extended author information available on the last page of the article

Introduction

The Late Pleistocene southern African archeological record provides the earliest evidence for the emergence of the complex symbolic and technological behaviors that characterize *Homo sapiens* (Henshilwood et al. 2004, 2009, 2018; Marean et al. 2007; Texier et al. 2010; McBrearty and Brooks 2000; Brown et al. 2009; Wadley 2015). To date, the bulk of research is at archeological sites located close to the current coastline (Smith et al. 2018; Marean et al. 2007; Henshilwood et al. 2011; e.g., Henshilwood et al. 2004; Wadley et al. 2011; Porraz et al. 2013; Wurz et al. 2018), and less work has thoroughly examined the record of early *Homo sapiens* in the deep interior savannah and grassland settings. Changing Pleistocene climates are often implicated as a significant driver of early human behavioral change (Ziegler et al. 2013; Deacon 1978; Mellars 2006; Mackay et al. 2014; Ambrose and Lorenz 1990; Foley and Lahr 1997; Marean 2015; Barham and Mitchell 2008), with a specific focus on the role of coastal and near-coastal environments and resources (Marean 2010, 2014; Smith et al. 2018; Parkington 2010; Will et al. 2019). However, the precise impacts of paleoenvironments on human behavior across much of Africa remain unknown, because the archeological record is geographically biased to these coastal settings.

We initiated investigations in the southern Kalahari Basin to address this geographical bias in current Late Pleistocene research. This region is ideal because recent discoveries from the Early and Mid-Pleistocene of the Kalahari Basin document early ages for many significant human innovations, including associations with fire (Berna et al. 2012), pigments (Watts et al. 2016), blade technologies (Wilkins and Chazan 2012), and stone-tipped spears (Wilkins et al. 2012), suggesting this area may have been an important locale for behavioral innovation in the past. Furthermore, it represents an interior ecotone environment at the edge of the Kalahari Desert that would have been highly susceptible to changes in past climate (Wasson et al. 2013), with probable shifts from productive savanna to arid/semiarid deserts with limited and patchy resources. Thus, the environmental context of the Kalahari Basin is in stark contrast to the more stable near-coastal environments with dense and predictable resources (Marean 2016).

Late Pleistocene sites have been documented and excavated in the Kalahari Basin and surrounding regions (Beaumont and Vogel 2006; Lukich et al. 2019; Porat et al. 2010; Humphreys and Thackeray 1983; Humphreys 1974; Kuman et al. 1999; Morris and Beaumont 2004; Beaumont and Morris 1990; Chazan et al. 2013; Forssman et al. 2010). However, previous excavations of Late Pleistocene deposits here generally provide lower-resolution data having been carried out prior to the regular use of total stations and advances in dating techniques and/or are at open-air sites with complicated taphonomic histories. Thus, current datasets and museum collections are limited in their capacity to address evolutionary questions.

Our project focuses on the region north of the town of Kuruman (Fig. 1), where few archeological investigations have taken place and systematic survey programs are likely to lead to the discovery of new sites. This area is also geologically significant; rockshelters and caves are rare in this part of southern Africa but occur in the Kuruman Hills along the contact between the Campbell Group dolomites and Kuruman banded ironstone formation (BIF). This contact is only exposed in a few places to the south of Kuruman, for example, at the location of Wonderwerk Cave, an important site with

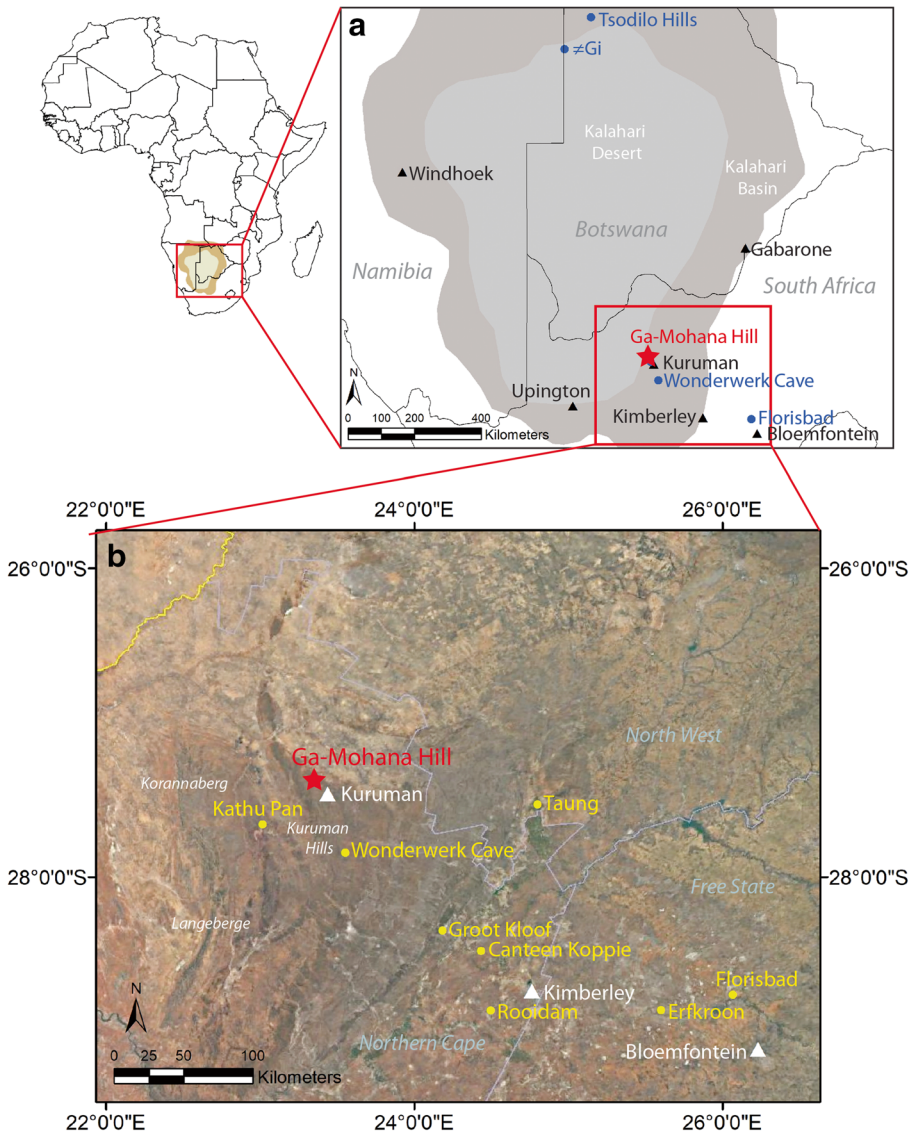


Fig. 1 Map of study area. **a** The location of Ga-Mohana Hill relative to the boundaries of the Kalahari Desert and Kalahari Basin and some well-known Stone Age sites (blue). **b** Location of Ga-Mohana Hill relative to local geographic features and Stone Age sites discussed in text (satellite imagery source: “Kuruman” – 27.47 N, 23.43 E. Google Earth. February 6, 2017. Accessed August 1, 2018)

well-preserved Early, Middle, and Late Pleistocene archeological deposits (Beaumont and Vogel 2006; Chazan et al. 2017). North of Kuruman, this dolomite-BIF contact is exposed in many places on the landscape, and consequently, there are many rockshelters that we have begun to systematically record and investigate.

Some small test excavations were carried out in the largest of these shelters, what we have called Ga-Mohana Hill North Rockshelter (GHN), by Thackeray and Thackeray (1980: 6–7). The only reported description amounts to a single paragraph, and there is

no known detailed report. The conclusion was that the entire deposit had been disturbed by guano diggers and through leveling the sediments for use as a cattle kraal. For this reason, no further archeological investigations were carried out.

Here we present the results of the first systematic excavation program at GHN, where we have recovered, analyzed, and dated the stratified Late Pleistocene Middle and Later Stone Age deposits. We investigate the extent to which the deposits have been subjected to postdepositional disturbance through stratigraphy, fabric analysis, and chronology.

Ga-Mohana Hill

Ga-Mohana Hill, also known locally as Ga Mohana, Gamohana, and Kurumankop, is a visually striking feature 12 km northwest of Kuruman on the eastern edge of the Kuruman Hills (Fig. 2). There are differing views on the most appropriate spelling, but Ga-Mohana is most in line with the SeTswana origin and is how many local people know it. Its meaning is likely “Of Mohana,” suggesting “Mohana’s place.” It is considered a place of significant spiritual importance (Maape 2016: 190–200).

The hill has a maximum elevation of 1531 masl, which is roughly 150–180 m above the surrounding landscape. The summit is composed of banded ironstone belonging to the Kuruman Member of the Griquatown Group. This overlays Campbell Group dolomite with interbedded chert and limestone belonging to the Gamohaam Formation (Gandin et al. 2005). Paleoproterozoic stromatolite fossils and other signs for early microbial marine life in the Gamohaam Formation have provided significant evidence for the processes that led to the oxygenation of our atmosphere (Gandin et al. 2005; Sumner 1997), meaning this specific exposure has been well studied. The contact between the upper Gamohaam Formation and the overlying Kuruman Member is gradational with interbedding of carbonate, shale, and iron formation (Sumner 1997). Sediments at the base of the hill are Quaternary rubble.

Rockshelters and overhangs occur at several places around the north, east, and west faces of Ga-Mohana Hill at similar elevations of roughly 1410–1430 masl within a relatively weaker band of the dolomitic Gamohaam Formation close to the contact with the overlying Kuruman Member.

GHN, the largest shelter on the hill, is a long, curved, and relatively shallow shelter (Fig. 2) facing to the northwest, with the viewshed including the Kuruman River to the north. The drip line is ~ 140 m across its entire width. The shelter outline can be divided into three main lobes, the central one being the largest in size and where we excavated.

Some of the shelters on the hill preserve rock paintings that are extensively weathered. These are finger-painted geometric forms in red, orange, yellow, and more rarely white pigments. The motifs commonly feature short parallel sets of vertical lines sometimes connected with a horizontal or curved line. In general, South African finger paintings are associated with more recent time periods, probably with the ceramic LSA and the last ~ 500 years (Beaumont and Vogel 1989; Van der Merwe et al. 1987).

On the lower slope of the north hill face, there is exposed dolomite in a small usually dry stream bed with several pecked rock engravings. These engravings are mainly geometric and complex curvilinear motifs with meandering lines that have been noted as snake-like (Beaumont and Morris 1990: 135–142). The artists and chronology of

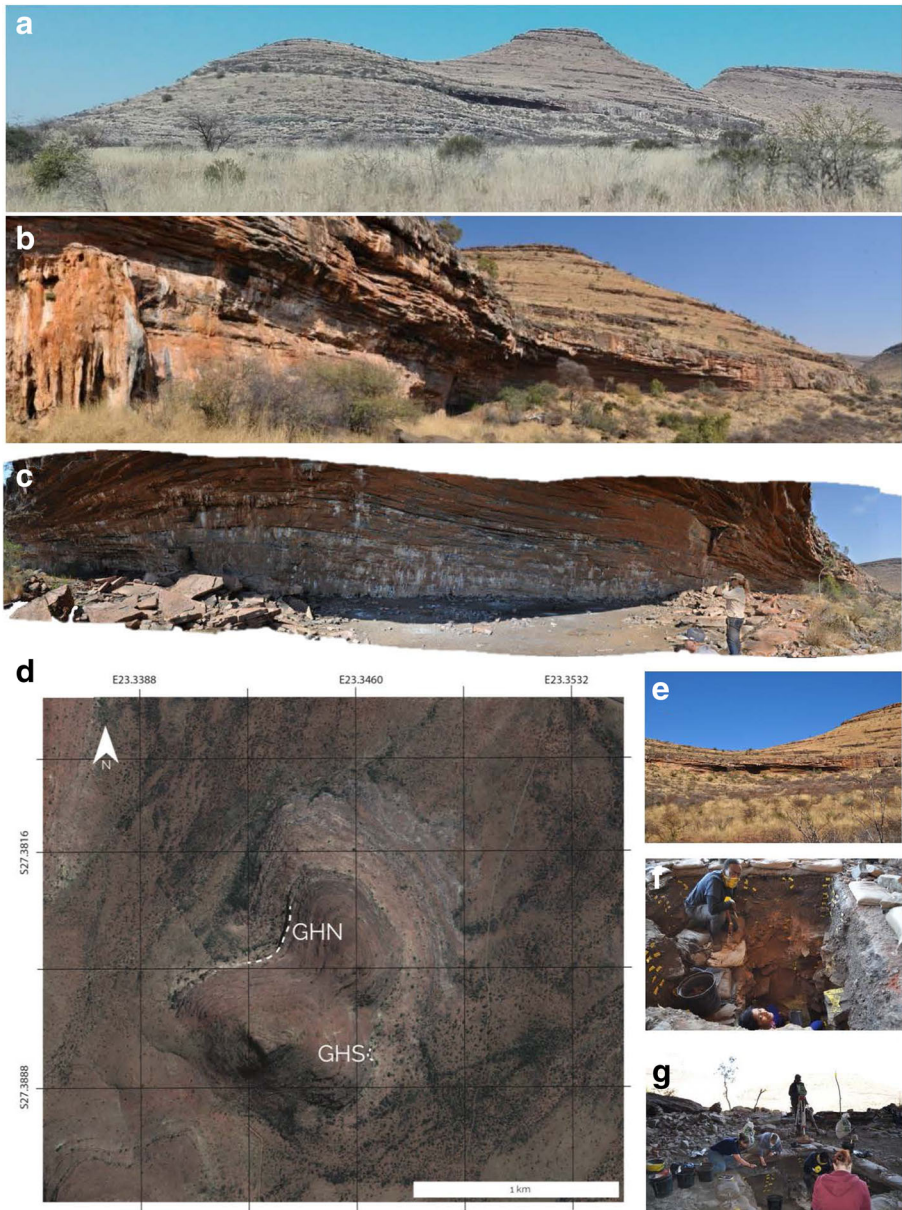


Fig. 2 Ga-Mohana Hill North Shelter (GHN). **a** View from northwest of Ga-Mohana Hill and GHN. **b** View from north end of shelter showing large tufa deposit on left side of frame. **c** Main lobe of GHN – panorama. **d** Birds eye view of Ga-Mohana Hill with locations of GHN and nearby Ga-Mohana Hill South Shelter (GHS) identified. **e** View from base of talus slope toward GHN. **f–g** Excavations at GHN

these engravings are debated. Engravings in the Kuruman River Valley at Batlharos appear to be associated with ceramic LSA and a radiocarbon date of 210 ± 30 BP (Beaumont and Vogel 1989). Other pecked engraving sites in the region depict Tswana-type shields and bilobial huts, ox-wagons, women in long dresses, and men on

horseback, confirming that at least some of the engravings are relatively recent (Beaumont and Morris 1990; Maggs 1995; Morris 1988). Adjacent to the engravings is a large rock gong consisting of four dolomite slabs with at least 18 hollows (Morris et al. 2018).

Methods

Excavations

Across three excavation areas at GHN (Fig. 3), we employed an excavation and plotting procedure modified from the one developed at the Pinnacle Point complex of archeological sites (Marean et al. 2004). We used an RTK GPS system to establish permanent control points on the bedrock and large roof fall at each site that are linked to the WGS84 UTM zone 34S grid so that all stratigraphic unit boundaries, cultural finds, sediment samples, section photos, and three-dimensional models could be tied to this grid using a total station.

Excavation areas are hierarchically organized by square, quadrant, and Lot. The 1×1 m² square is named for the northeast corner's last three digits before the decimal place of the UTM coordinates. Each square is divided into four quadrants based on cardinal directions (NE, NW, SE, SW). Minimal excavation units are numbered "Lots." Lots that show similar sedimentary characteristics are then grouped into alphabetic units and then stratigraphic aggregates that are named based on the unifying sedimentary traits. Where no sedimentary change was encountered, lots were arbitrarily split into 5-cm spits. All sediments were dry-sieved on site through a nested 10 mm-3 mm-1.5 mm sieve set.

We piece plotted all visible artifacts with no size cutoff. For most artifacts, a single measurement is taken at the center of the artifact base. Two sets of coordinates are collected for all artifacts > 15 mm in maximum length with a clear long axis at the base of either end. This permits the calculation and visualization in GIS of artifact orientation and dip (Bernatchez 2010; McPherron 2005, 2018; Oestmo et al. 2014). A size cutoff for collecting two-shot data was employed to account for total station error of ~ 10 mm. Bulk sediment samples were collected from each lot. All material is currently under continued study at the University of Cape Town, but will be curated at the McGregor Museum, Kimberley.

Nineteen (19) quadrants across three excavation areas were excavated (4.75 m²). Area A (4 m²), located in the southern portion of the main lobe, is the largest and deepest excavation area to date and is the focus of this manuscript.

Artifact Analysis

All plotted finds from Area A ($n=2128$) were cataloged by major class (lithic, fauna, ostrich eggshell (OES), charcoal, other). Here, we present a qualitative overview of the excavated material. Material from the sieves is still being sorted from the abundant natural roofspall; thus, a complete analysis of all excavated material will only be presented once this post-excavation processing is complete.

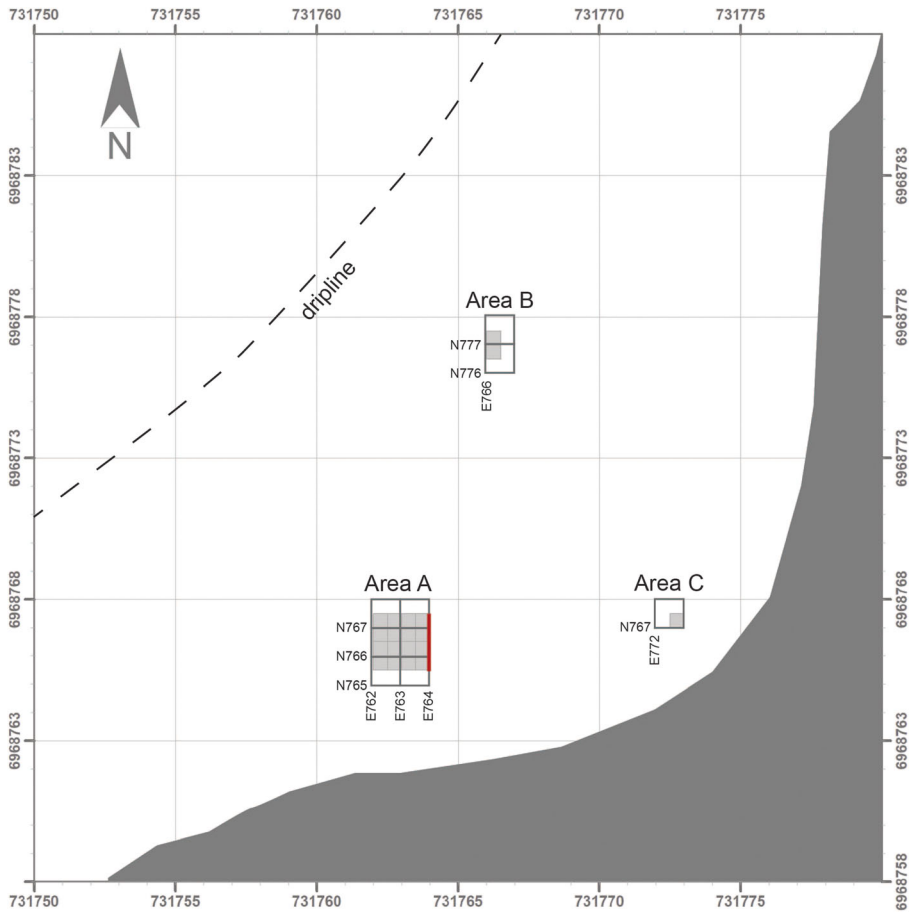


Fig. 3 Excavated areas at GHN. Excavated quadrants (0.25 m^2) are shown in gray. Square names are based on the coordinates of the southwest corner. Red line marks profile shown in Fig. 4 (E764 line)

Fabric Analysis

Patterns in the artifact orientation and slope data are explored here using a combination of approaches drawn from McPherron (2005, 2018), Dibble et al. (1997, 2006), Bernatchez (2010), Lotter et al. (2016), and Oestmo et al. (2014). Orientation, or bearing, is calculated using the two-shot data on elongated artifacts and a $0\text{--}360^\circ$ scale after McPherron (2005). The slope of the artifact, or its plunge, was calculated on a $0\text{--}90^\circ$ scale. Data was visually assessed with ArcGIS 10.2. Artifacts with slope and orientation data were projected horizontally and vertically as lines using the 3D Character Marker option. The value for marker size (y-axis) was set at $10 \times$ width and depth with the “vertical orientation” option unchecked. The orientation value for each artifact was set as the value for rotation around the z-axis and the slope value for rotation around the x-axis. Slope for each unit with an adequate sample size is presented as a histogram of values between 0 and 90° using Oriana 4.02 software. A Kolmogorov-Smirnov (KS) test is used to establish the probability that the distribution

is uniform using Past 3.06 software (Hammer et al. 2001). The uniform distribution is generated on a scale of 0–90° with the same sample size as the test distribution. Orientation data was summarized using Rose diagrams generated with Oriana 4.02. Our sample sizes range from $n = 8$ to $n = 118$. With the same program, the Rayleigh test of uniformity for circular data was used to determine whether the orientations have a tendency to cluster. We used a significant level of 0.05 for all tests.

The expectation for undisturbed artifacts is that they are randomly oriented and not significantly different from a uniform distribution. Postdepositional processes tend to introduce patterning in orientation (McPherron 2005; Schiffer 1987). Undisturbed artifacts will also exhibit slopes that follow the sediment surface, which is near 0° on a horizontal surface, and the distribution will be significantly different from a uniform distribution.

Another method for statistically summarizing an assemblage of artifact orientation data is by plotting two ratios calculated from the first three eigenvalues of orientation and plunge values (Benn 1994). The ratios of these eigenvalues are calculated as an “isotropy index” and an “elongation index.” When scaled onto a ternary plot, Benn diagrams display the relative association of an assemblage to three orthogonal vectors describing formation processes at each of the corners. At the top of the ternary diagram are isotropic fabrics where clasts are oriented randomly in both horizontal and vertical dimensions. In the lower right corner are clasts oriented in roughly the same direction on a linear fabric. In the lower left corner of a Benn diagram are objects in a planar fabric configuration, meaning random orientation on a flat surface such as an idealized archeological surface. Clasts from known disturbance processes described by Lenoble and Bertran (2004) provide a visual reference for identifying the assemblage affinity to known geologic processes such as water runoff and debris flows. For a more quantitative assessment of whether assemblages are significantly different on a Benn diagram, McPherron (2018) developed a permutation test that provides a 95% confidence interval in Benn diagram space by resampling each assemblage 10,000 times and plotting the contour line that contains 95% of the permuted indices. An additional pairwise p value for each set of layers is calculated by comparing the observed difference against a permutation of the two assemblages combined without replacement 10,000 times. The methods presented by McPherron (2018) were adapted for the StratAggs and linear concentrations at Ga-Mohana using the R statistical programming environment, and the code is available in Online Resource 1.

Geochronological Analyses

Three (3) charcoal samples excavated from Area A at GHN were sent for accelerated mass spectrometry (AMS) radiocarbon analysis. These samples underwent acid-base oxidation (ABOx) (Bird et al. 1999) or a modified acid oxidation (AOx) (Douka et al. 2019). Our samples were split between two laboratories: the Beta Analytic AMS Laboratory, Miami, USA, and the Oxford Radiocarbon Accelerator Unit (ORAU), UK. Calibration was performed using OxCal v. 4.3.2 and the SHCal13 calibration curve (Hogg et al. 2013).

Five (5) samples for single-grain optically stimulated luminescence (OSL) dating (Huntley et al. 1985; Rhodes 2011) were collected by hammering stainless steel tubes (5-cm diameter) into cleaned sections. Standard preparation procedures were used

(following Gliganic et al. 2017) to isolate quartz grains of 180–212- μm diameter. Grains were loaded into a Risø TL/OSL DA20 reader and stimulated for 2 s at 125 °C with a green laser (532 nm) (Botter-Jensen et al. 2003), and the ultraviolet OSL emission was measured using an Electron Tubes Ltd. 9635Q photomultiplier tube through 7.5 mm of Hoya U340 filter. Signals were calculated by summing the first 0.17 s of signal and using the final 0.3 s to calculate background. Equivalent dose (D_e) values were estimated using the single-aliquot regenerative dose (SAR) procedure (Murray and Wintle 2000) with natural/regenerative and test dose preheats of 220 °C for 10 s and 220 °C for 5 s, respectively. Standard tests of SAR suitability included a dose recovery experiment, recuperation test, recycling ratio test, and OSL-IR depletion ratio test. D_e distributions were analyzed using the Central Age Model (CAM, Galbraith et al. 1999) and the Finite Mixture Model (FMM, Roberts et al. 2000). Beta and gamma dose rates for samples were estimated using GM-25-5 beta counting (Botter-Jensen and Mejdahl 1988), thick-source alpha counting, and the conversion factors of Guérin et al. (2011). Samples GHN6 and GHN2 were collected close to bedrock, and sample GHN5 was collected close to the surface, so the gamma dose rate contributions for these samples were modeled to take this into account (Aitken 1985). The cosmic-ray dose rate was calculated following Prescott and Hutton (1994), and an internal alpha dose rate of 0.03 ± 0.01 Gy/ka was assumed. A water content of $5 \pm 2.5\%$ was used to allow for past variations in the soil moisture, so as to calculate dose rate attenuation by moisture.

A small 3-cm tubular stalactite (soda straw fragment) excavated from Area A at GHN was dated using U-Th. Standard U-Th dating procedure was carried out following laboratory protocols detailed by Hellstrom (2003, 2006) at the University of Melbourne. U-Th isotope-ratio measurements were performed on a Nu Instruments Plasma Multi Collector-Inductively Coupled Plasma-Mass Spectrometer (MC-ICP-MS) following the procedure of Hellstrom (2003).

Results

Stratigraphy

Excavations at Area A revealed 170 cm of stratified archeological deposits with abundant lithic and faunal artifacts. From surface to a depth of about 10 cm, sediments are loose, with laterally limited patches of dung- and charcoal-rich sediments. Below these surface sediments are three other stratigraphic aggregates from top to bottom: dark brown gravelly silt (DBGS), orange ashy silt (OAS), and dark brown silt and roofspall (DBSR) (Fig. 4).

DBGS The DBGS is characterized by subrounded to rounded gravels, approximately 20 mm in size or less, with variable inputs from roofspall. The DBGS gravels are dolomite and chert and seem to derive from the hillslope above the shelter. The sediment is clast supported with a silt matrix and 40–50 cm thick. Grassy organics occur throughout the DBGS but are highly concentrated in a few patches. The lower 20 cm has larger and greater frequency of roofspall inclusions than the upper levels. Within the DBGS, there are some loose patches with voids between the clasts and

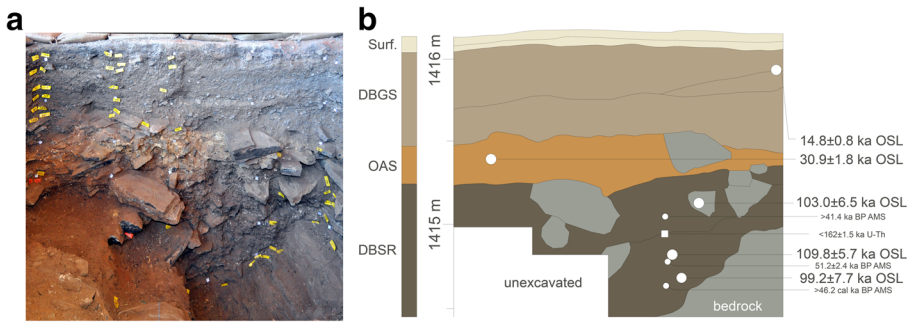


Fig. 4 Stratigraphy of Area A at GHN. **a** Georeferenced section photo of east wall, E764 line. **b** Schematic of stratigraphic boundaries, stratigraphic aggregate assignments, and radiocarbon, OSL, and soda straw sample locations and results. Gray-shaded areas are rock

burrows. These are concentrated in the western part of the excavation area and were excavated as separate Lots. There is vertical variability within the DBGS (Fig. 4), with the lower stratigraphic levels containing a higher frequency and larger roofspall clasts with less of a silt component.

OAS The OAS is a visually striking orange loosely compacted silt deposit with roofspall and gypsum inclusions. The roofspall inclusions are often blackened, and there are some blackened patches of sediment within the OAS. The OAS exhibits variable thicknesses across the sections, from 10 to 30 cm. The upper surface of the OAS is wavy and occurs at various elevations across the excavation area. The contact with underlying DBSR is sharp and mainly horizontally bedded.

DBSR The DBSR is an ashy matrix supported deposit with roofspall and gypsum inclusions varying in size up to 35 cm. Like the overlying OAS, many of these roofspall fragments are blackened. There are patches of charcoal throughout DBSR. Roofspall size and frequency vary vertically through the DBSR, with larger sizes and higher frequencies in the upper 20 cm of the deposit. Loose sediments with lots of organic material, identified as a burrow, were encountered in the eastern portion of the excavation area. These sediments were excavated as a separate Lot. There are several lenses throughout the DBSR with small angular gravels, and gypsum content varies as one moves down the section. The DBSR is the lowermost excavated unit. It is up to 80 cm thick in the eastern portion of the excavation area where it directly overlies bedrock that slopes sharply down to the north.

Archeological Sequence

Below is a brief overview of the artifact types recovered from each stratigraphic unit. The assemblages exhibit uniformity within each stratigraphic aggregate. The results of detailed analyses are forthcoming.

Surface The surface sediments at GHN contain rare historical debris, including glass fragments and European refined earthenware fragments.

DBGS Artifact density is relatively low in the DBGS compared to the lower stratigraphic aggregates and includes lithic and faunal artifacts, OES fragments, OES beads, and bead preforms (Table 1). The DBGS lithic assemblage includes bladelets, bladelet cores, and rare backed pieces. These lithic artifact types, together with the OES beads and bead preforms recovered from this unit, are consistent with a Later Stone Age designation. The lithic artifacts at GHN are primarily manufactured on chalcedonic black chert, dark gray-green tuff, banded ironstone, quartz, and chalcedony. Most of these materials are abundant and available locally. Black chalcedonic chert occurs as thick layers, within the dolomitic Gamohaana Formation that the shelter has formed within. Banded ironstone formation outcrops at the summit of Ga-Mohana Hill, and nodules are abundant on the talus slope and in the valleys at the base of the hill. The tuff outcrops above the rockshelters as a 30–40 cm thick layer within the dolomitic Gamohaana Formation (Sumner and Bowring 1996). Quartz seams and large well-formed quartz crystals within the dolomite at Ga-Mohana are also observed. Chalcedony has not been observed on the landscape near the shelters, but it occurs in limited frequencies in drainage systems ~40 km to the west (Wilkins 2017). Faunal material recovered through the GHN sequence is fragmentary, but in many cases, the surfaces are moderately preserved, and some larger fragments are identifiable to element and higher order taxa. Faunal finds in the DBGS include tortoise, size class 1–4 (Brain 1981) ungulates, and a molar identified as red hartebeest.

OAS Stratified below the LSA-bearing DBGS is the OAS. The shift in artifacts is dramatic, with the OAS representing a flake- and blade-based industry made primarily on tuff and chalcedonic black chert, with a moderate frequency of retouched tool types that includes unifacial points, notched pieces, and scrapers. The assemblage also includes unretouched points, prepared cores, and prepared platform flakes and blades, consistent with an MSA designation. Artifact density is moderate relative to other stratigraphic aggregates at GHN (Table 1). OES fragments and beads are absent in our current sample of the OAS. Fauna remains are highly fragmented, but identifiable specimens include tortoise and size class 1–4 ungulates.

DBSR Artifact density in the DBSR is relatively high relative to the overlying stratigraphic aggregates (Table 1). The lithic assemblage of the DBSR contains very large points, blades, and prepared cores, consistent with an MSA designation. Compared to the overlying OAS, the DBSR exhibits more chalcedonic black chert and banded ironstone and fewer retouched tools. The faunal remains also include tortoise and size class 1–4 ungulates. Cut marks and percussion marks are preserved on several of the DBSR specimens. OES fragments (unmodified) exhibit a relatively high frequency in this stratigraphic aggregate relative to others; beads are absent (Table 1).

Fabric Analysis

Artifact plotted find coordinate data for Area A is available in Online Resources 2 and 3.

Consistent with minimal disturbance, few artifacts deviate far from a slope of zero in all stratigraphic aggregates (max mean value = 17.33°), and they differ significantly

Table 1 Summary of the volume of excavated sediment (L), recovered artifact types (plotted finds only), and artifact density (n/L) by stratigraphic aggregate in Area A at GHN

StratAgg	Volume Exc. (L)	Lithic		Fauna		OES		Charcoal		Other		All	
		n	Density (n/L)	n	Density (n/L)	n	Density (n/L)	n	Density (n/L)	n	Density (n/L)	n	Density (n/L)
Surface	114	51	0.45	14	0.12	12	0.11	1	0.01	5	0.04	83	0.73
DBGS	1278	271	0.21	159	0.12	52	0.04	16	0.01	34	0.03	532	0.42
OAS	265	133	0.50	153	0.58	0	0.00	1	0.00	14	0.05	301	1.14
DBSR	431	625	1.45	482	1.12	52	0.12	3	0.01	50	0.12	1212	2.81
Total	2088	1080	0.52	808	0.39	116	0.06	21	0.01	103	0.05	2128	1.02

Volume of excavated sediment was calculated based on number of full 9-L buckets. OES ostrich eggshell. The Other category includes organic material, carbonates, rare ochre fragments, quartz and calcite crystals, and unidentifiable items

from a uniform distribution (Table 2; Fig. 5). Also consistent with minimal disturbance, artifact orientations are not preferential and do not differ significantly from a uniform distribution for all analyzed stratigraphic aggregates (Table 2; Fig. 6).

The 95% confidence interval around each stratigraphic aggregate on a Benn diagram is shown in Fig. 7. The DBGS and OAS fall near the planar corner largely outside of the comparative geologic processes from Lenoble and Bertran (2004), consistent with expectations for minimal postdepositional disturbance. The surface sediments plot nearly directly on the planar–linear axis of the ternary diagram, suggesting very little variability in plunge of these artifacts (as would be expected on the surface). The DBSR plots within the shallow runoff process. Overall, none of the layers are significantly different from each other based on this sample (Table 3).

Geochronological Analyses

The three radiocarbon samples originated from the DBSR (Fig. 4). They support a Pleistocene age for the lowest deposits at GHN, indicating that the DBSR in Area A dates to minimally ~44 ka (Fig. 4; Table 4). A conservative interpretation is that all age estimates resulting from these samples are minimum values given their proximity to the limits of radiocarbon dating.

Five OSL samples were collected and measured from GHN (Fig. 4): three from the lowest DBSR unit (GHN6, GHN2, and GHN3), one from OAS (GHN4), and one from DBGS (GHN5). Equivalent dose and dose rate data are shown in Table 5. A typical decay curve and dose-response curve are shown in Fig. 8. Measured/given dose ratio results from single-grain dose recovery tests using given doses of 46 and 93 Gy are consistent with unity, showing that the SAR procedure can accurately estimate known radiation doses for these samples. CAM overdispersion values range between 28 and 78%, with some samples having overdispersion values larger than those expected based on dose recovery experiments or intrinsic factors (i.e., Thomsen et al. 2012). To identify the age model that best fits each De distribution, a systematic approach was used. This approach uses stratigraphic position and environmental context of samples, the overdispersion of CAM and FMM results, and two statistical measures (the maximum log likelihood and the Bayes information criterion: Roberts et al. 2000; Jacobs et al. 2008) to determine the model that best fits each De distribution and the De values that best represent deposition of the sediments (Cohen et al. 2015; Gliganic et al. 2015). The depositional ages for GHN5 and GHN4 are 14.8 ± 0.8 ka and 30.9 ± 1.8 ka. The three ages for DBSR are 103.0 ± 6.5 ka, 109.8 ± 5.7 ka, and 99.2 ± 7.7 ka. While the

Table 2 Summary statistics of artifact slope and orientations in degrees at GHN by stratigraphic aggregate

StratAgg	<i>n</i>	Slope Mean	SD	D (K-S test)	<i>p</i>	Orientation Mean vector	Circular SD	Rayleigh Z	<i>p</i>
Surface	8	6.79	5.53	0.75	0.010	26.14	83.46	0.96	0.396
DBGS	81	10.39	11.18	0.68	<0.001	25.18	135.21	0.31	0.734
OAS	61	7.59	6.08	0.75	<0.001	251.25	109.34	1.60	0.202
DBSR	118	9.75	11.02	0.69	<0.001	276.95	134.54	0.48	0.622

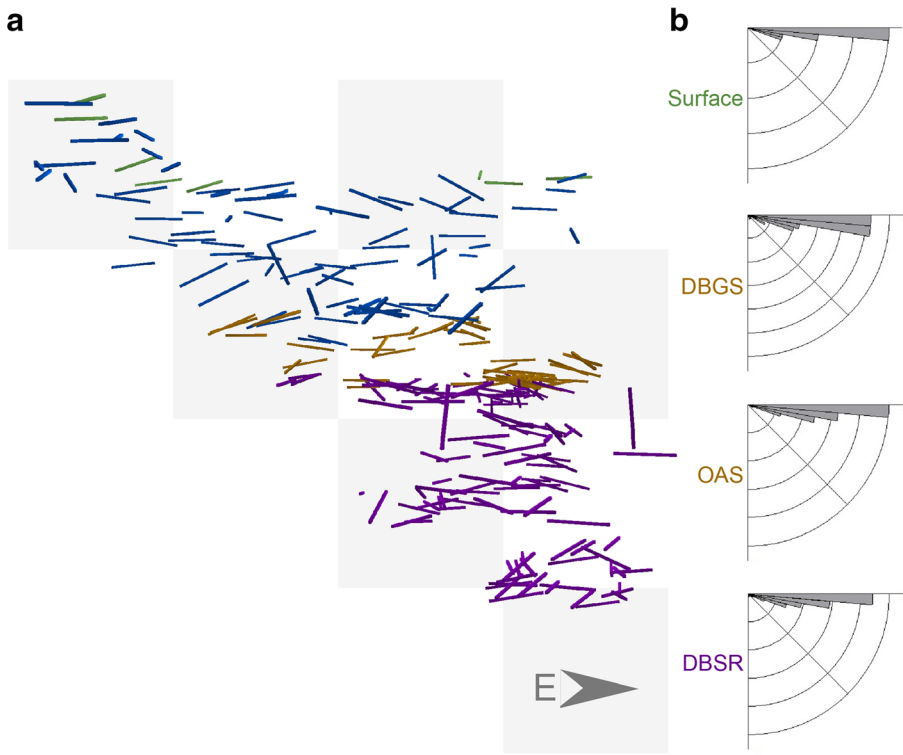


Fig. 5 Plotted find slopes in Area A at GHN. **a** Plotted finds with two-shot data displayed in 3 dimensions and color-coded by stratigraphic aggregate assignment: purple = DBSR, orange = OAS, blue = DBGS, green = surface sediments and dung. **b** Rose diagrams of slope by stratigraphic aggregate

depositional ages for these three samples range by ~ 10 ka, standard statistical homogeneity testing shows that they are consistent with a common value (95% confidence level, Galbraith 2003), which is best represented by the weighted mean age of 105.3 ± 3.7 ka for the DBSR unit. The concordance of three depositional ages indicates that the DBSR unit was deposited over a relatively short time period.

The tubular stalactite fragment recovered from the DBSR (Fig. 4) gave a U-Th age of 162 ± 1.5 ka. This provides a maximum age estimate for the sediments and associated artifacts, indicating the age of the formation of the stalactite, and not when it was incorporated into the deposit. This result is consistent with the ~ 105 -ka age estimate for the DBSR based on OSL.

Discussion

Previous reports suggested that kraal construction and/or guano digging had disturbed the sediments at GHN (Thackeray and Thackeray 1980). Contrary to this report, our investigations demonstrate that there are well-preserved, intact MSA and LSA deposits in the shelter. These deposits are chronometrically dated to the Late Pleistocene using OSL analysis. For the oldest deposit (DBSR), infinite radiocarbon age estimates on

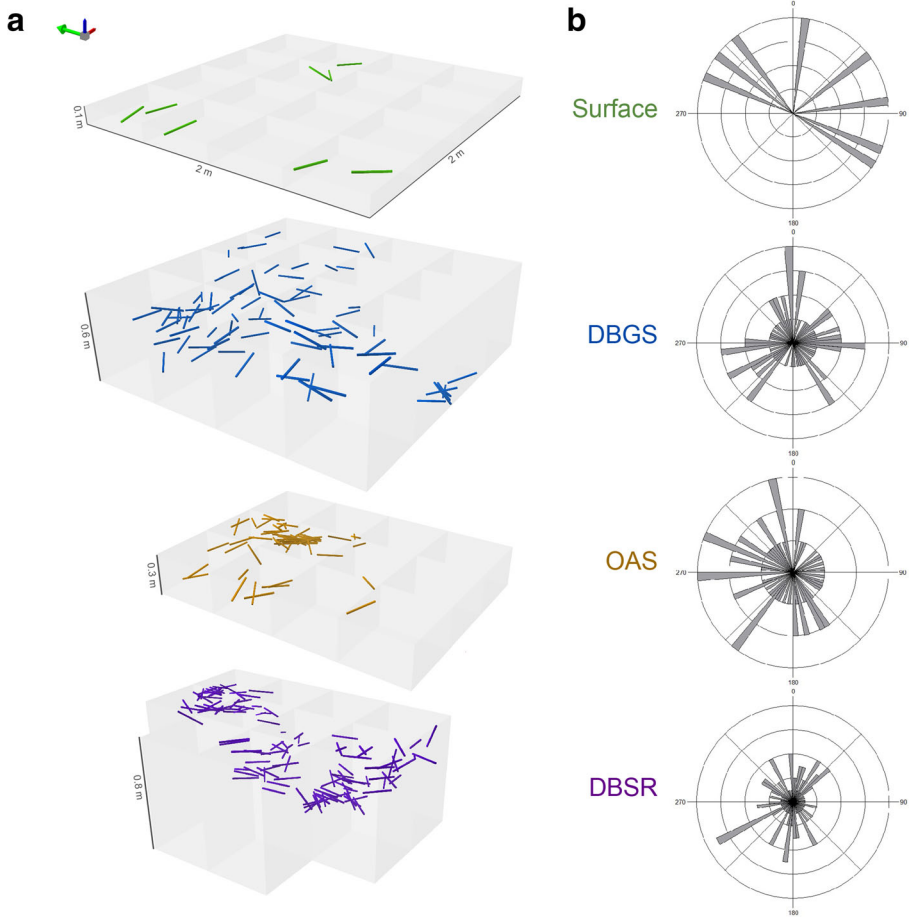


Fig. 6 Plotted find orientations in Area A at GHN (profile view toward north). **a** Plotted finds with two-shot data displayed in 3 dimensions and by stratigraphic aggregate. **b** Rose diagrams of orientation by stratigraphic aggregate

charcoal and a maximum age estimate of ~ 162 ka based on a tubular stalactite are consistent with the OSL result. The record of occupation in Area A at GHN appears punctuated, represented by three subsurface stratigraphic aggregates DBSR, OAS, and DBGS, dating to ~ 105 ka, ~ 31 ka, and ~ 15 ka, respectively. Cultural artifact distributions are consistent with an LSA assemblage in the DBGS, which overlays two stratified MSA assemblages (OAS and DBGR), with no evidence for significant disturbance or mixing.

The strongest supporting evidence for in situ deposits that have experienced minimal disturbance comes from the detailed fabric analysis presented here that shows the artifacts mainly lay flat within the horizontally bedded sediments, they exhibit non-preferential orientations, and they plot mainly within the minimal slope wash zone of a Benn diagram.

We encountered bedrock at a depth of 120 cm below surface in the northeast corner of excavation Area A. Continued excavations toward the front of the shelter reached a

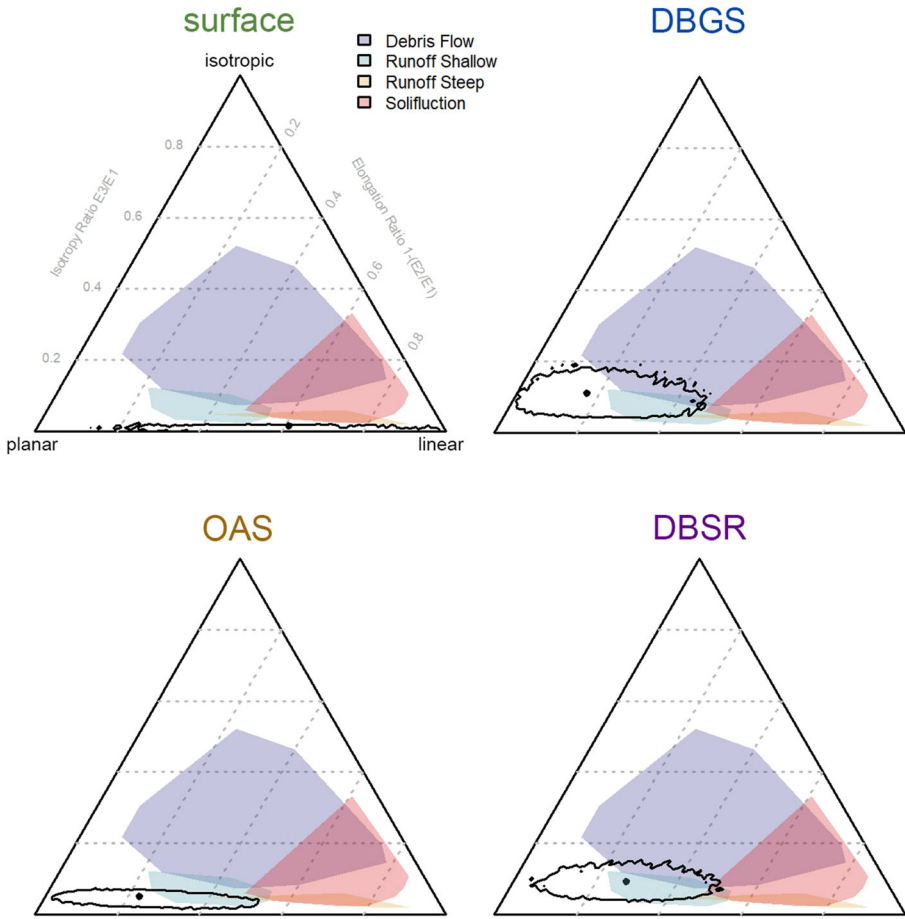


Fig. 7 Benn diagrams by stratigraphic aggregate in Area A at GHN showing 95% confidence intervals. The dot at the center of the contour indicates the observed Benn indices value for that stratigraphic aggregate. The contour line indicates the extent of a 0.95 probability line from the permutation test

depth of 173 cm without hitting bedrock, indicating that the bedrock slopes steeply down in that direction. For this reason, we suspect that the deposits may be deeper near the front of the shelter, potentially preserving yet older deposits as excavations continue.

Establishing good context at Ga-Mohana Hill is especially important before investing further effort in excavation, given that contextual issues have been a

Table 3 *p* values associated with permutation test of pairwise comparisons of stratigraphic aggregate fabrics

	DBGS	OAS	DBSR
Surface	0.1805	0.1998	0.3335
DBGS	–	0.5635	0.4705
OAS	–	–	0.7441

Table 4 Results of AMS radiocarbon analysis on three charcoal fragments from DBSR in Area A at GHN

Specimen ID	Lab ID	Pretreatment protocol	Isotopes results (o/oo)	Radiocarbon age	Calibration result (2 sigma, 95% prob)
PF 1889	Beta-456294	ABOx	- 22.7	40,620 ± 280 BP	cal BP 44750–43,500
PF 1889	OxA-35956	AOx	- 21.1	> 41,400 BP	n/a
GHN10 3 mm Lot 150	OxA-35861	AOx	- 23.1	51,200 ± 2400 BP	n/a
PF 2200	Beta-456295	ABOx	- 22.2	> 43,500 BP	> cal BP 46150

Specimen PF 1889 was split into two halves, with one half analyzed by Beta Analytic AMS Laboratory, Miami, USA, and the other at the Oxford Radiocarbon Accelerator Unit (ORAU)

limitation for MSA deposits in the southern Kalahari Basin. For example, the MSA deposit at Kathu Pan 1 is in secondary context within a gravely matrix, and the artifacts show evidence of having been water-worn and rolled (Beaumont and Morris 1990; Porat et al. 2010). There is also some ambiguity about the context of the speleothems in the MSA levels at the region's flagship site, Wonderwerk Cave, and what they indicate about the age of the associated artifacts (Herries 2011). Furthermore, while the artifacts recovered from earlier excavations at Wonderwerk Cave are well-provenienced with respect to square and depth below surface, this is a coarse-grained resolution given new advances in geospatial information technologies and limits the capacity to assess site formation processes. Current investigations at Kathu Pan and Wonderwerk are focused on resolving some of these limitations (Lukich et al. 2019; Horwitz and Chazan 2015; Ecker et al. 2017; Chazan et al. 2017). Our discovery of in situ MSA and LSA deposits at GHN presents an additional opportunity for investigating human behavioral evolution in the southern Kalahari Basin using excavation and analytical techniques that provide high-resolution data.

The DBGS assemblage at GHN adds to the growing record of MIS 2 occupation across southern Africa, expanding the range of human occupation deeper into the semiarid southern Kalahari Basin. Sites chronometrically dated to MIS 2 have been identified to the east and south of GHN, at Kathu Pan 5 (Beaumont and Morris 1990), Wonderwerk Cave (Beaumont and Vogel 2006), Dikbosch 1 (Humphreys and Thackeray 1983; Humphreys 1974), Equus Cave (Beaumont and Morris 1990), and Erfkroon (Palmison 2014; Tooth et al. 2013), hinting at a relatively substantial hunter-gatherer presence in the region during this time. MIS 2 technologies have been presented as adaptive solutions to environment degradation, representing a highly mobile hunter-gatherer strategy with large ranges (Ambrose and Lorenz 1990; Deacon 1976) and increased interaction that serves to reduce risk (Bousman and Cruz-Uribe 1998) in light of unpredictable resources (Mackay et al. 2014). Our results show that MIS 2 occupation in the southern Kalahari Basin is more extensive than generally recognized, extending into regions with relatively high aridity today, and may attest to extensive social networks across southern Africa during that time.

Southern African “final MSA” assemblages of late MIS 3 show localized technological patterning, which could reflect a more fragmented social landscape (Mackay et al. 2014). The OAS assemblage at GHN documents this variability further, with a new perspective from the southern Kalahari Basin. Characterized by large points and

Table 5 Results of OSL dating at GHIN

Sample	Water content (%)	Dose rate (Gy/ka)		Equivalent dose			Age (ka)						
		Beta	Gamma	Cosmic	Total*	n=		Overdispersion	Age model	FMM OD	FMM k	Proportion	De (Gy)
GHN 5 (DBGS)	0.3	0.92 ± 0.04	0.40 ± 0.01	0.06 ± 0.01	1.40 ± 0.06	183	28 ± 2	CAM		1.00		20.7 ± 0.5	14.8 ± 0.8
GHN 4 (OAS)	1.6	1.52 ± 0.07	0.70 ± 0.02	0.06 ± 0.01	2.31 ± 0.11	344	48 ± 2	FMM	0.30	2	0.82	71.4 ± 2.1	30.9 ± 1.8
GHN 3 (DBSR)	1.2	1.44 ± 0.07	0.65 ± 0.02	0.05 ± 0.01	2.18 ± 0.10	346	49 ± 3	FMM	0.22	3	0.67	224.2 ± 8.2	103.0 ± 6.5
GHN 2 (DBSR)	1.9	1.64 ± 0.07	0.73 ± 0.02	0.05 ± 0.01	2.40 ± 0.10	386	37 ± 2	FMM	0.26	2	0.94	263.9 ± 5.7	109.8 ± 5.7
GHN 6 (DBSR)	1.1	2.16 ± 0.10	0.96 ± 0.02	0.05 ± 0.01	2.56 ± 0.12	340	78 ± 4	FMM	0.36	3	0.59	253.7 ± 14.4	99.2 ± 7.7

Dose rate, equivalent dose, and age data for OSL samples are shown. See text for details of dose rate and equivalent dose measurement and calculation. Uncertainties are reported at the 68% confidence level

*Includes an internal dose rate contribution of 0.03 ± 0.01 Gy/ka

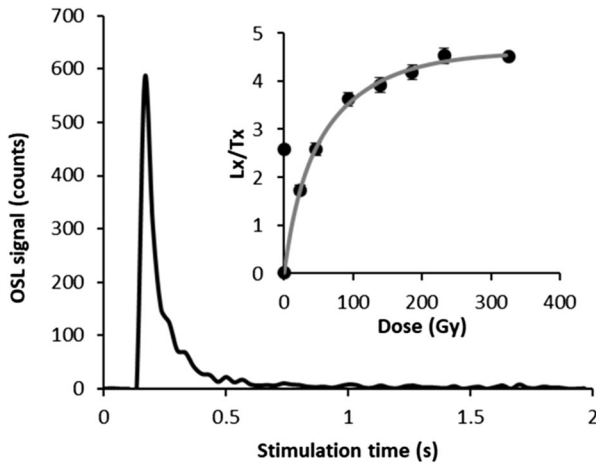


Fig. 8 OSL decay curve (Tn) from a representative grain of sample GHN6. Inset shows the corresponding dose-response curve

blades, and lacking substantial evidence for bipolar percussion, bladelet production, and bifacial points, the OAS assemblage differs from many other late MIS 3 assemblages in southern Africa. This includes, for example, the distant sites of Rose Cottage Cave (Soriano et al. 2007), Sibudu Cave (Villa et al. 2005; Wadley 2005), Umhlatuzana (Kaplan 1990), Umbeli Belli (Bader et al. 2016, 2018), Sehonghong (Pargeter and Redondo 2016) to the east, #Gi (Brooks et al. 1990), White Paintings Rockshelter (Robbins et al. 2000) to the north, and Putslaagte 8 to the southwest (Low and Mackay 2016). It also differs from the roughly coeval assemblage at Kathu Pan 5 only ~60 km to the southwest, where a lithic assemblage described as “early LSA” is associated with OES beads (Beaumont and Morris 1990). This variability is in line with the fragmented social landscape hypothesis.

The DBSR assemblage at GHN is one of very few in the southern Kalahari Basin to be chronometrically dated to early MIS 5. At Wonderwerk Cave, Major Unit 2 contains MSA-type artifacts and is presented with an age range between ~73 and ~220 ka based on U-Th dating of speleothem (Beaumont and Vogel 2006); thus, some of the assemblages there may be coeval with the DBSR at GHN. However, it is not clear whether the dated speleothem is broken fragments or in situ growths (Herries 2011). If we assume the speleothem are fragments and not found as in situ growths, then each provides a maximum age for the deposit they were recovered from (Herries 2011), indicating that all of Major Unit 2 is likely younger than ~220 ka, and some of the deposit is younger than ~73 ka. At Kathu Pan 6, a Howieson’s Poort-designated deposit has yielded OSL age estimates of 74 ± 5 ka and 100 ± 6 , the latter putting it coeval with the DBSR at GHN despite major differences in lithic technology (Lukich et al. 2019). Besides Wonderwerk Cave and Kathu Pan, the nearest roughly coeval occupation is at Florisbad, where points and prepared cores occur in primary/near primary context at an open-air site on a paleolake margin and are associated with an ESR age estimate of 121 ± 6 ka (Grün et al. 1996; Kuman et al. 1999). Although located more than 300 km apart, Florisbad and GHN will provide a useful temporal comparison because open-air and rockshelter sites sample different aspects of a mobile

foraging strategy. Rockshelters are rare in the interior of South Africa beyond the Cape Fold Belt and Drakensberg but often have better preservation than open-air sites and can be the foci for a greater range of daily activities than any single open-air site (Barton and Clark 1993; Binford 1982). As a rockshelter site chronometrically dated to ~105 ka, GHN adds an important point of reference for MSA behavior in the deep interior of southern Africa.

Rockshelters offer protection from the elements in an otherwise open and exposed landscape. GHN also offers an excellent vantage point, offering uninterrupted views of the Kuruman River Valley to the north and the Ghaap Plateau to the east. These qualities of the space have the potential to serve both the day-to-day physical needs of foragers, as well as inspiring use of the space for ritual activities, as it does today (Maape 2016). Water availability may have also drawn hunter-gatherers to Ga-Mohana Hill. Small amounts of water seep out of crevices in some of the shelter walls, even in mid-winter, water collects in natural pools in the dolomitic bedrock near the base of the hill after rainfall, the Kuruman River is 3 km away, and the Eye of Kuruman (a massive historically significant fresh water spring) is 12 km away.

Conclusion

The results of the analyses presented here indicate the high potential of GHN as a rich archive of MSA hominin behavior in the Kalahari Basin. Investigations at GHN are also embedded within the larger research program aimed at recording Stone Age archeology across the landscape and investigating paleoenvironments. Future research at GHN will leverage its position in an ecotone environment at the edge of the Kalahari Desert and its well-preserved datable deposits. Specific goals include expanding the excavation areas, further dating analyses, detailed materials analysis of the artifacts, and paleoenvironmental investigations through various proxies (the abundant tufa style carbonates and the associated fauna). With these data, we will be able to investigate how climatic fluctuations altered the southern Kalahari landscape in the Late Pleistocene and how humans in this area adapted to these changes. For the first time, in an area where we know ESA hominins thrived but where little is known about the Late Pleistocene, we will be able to generate a record that can be compared with better known records from other regions and test evolutionary hypotheses about the origins and evolution of our species.

Acknowledgments We acknowledge and pay respects to the traditional owners of the land on which GHN is located. Thank you to the Baga Motlhwane Traditional Council for the permission to work at Ga-Mohana. We would also like to thank David Morris, Kgosi P.P. Toto, Simon Hall, Michael Chazan, Curtis Marean, Peter Beaumont, Andy Herries, Nicholas Zachariou, Tessa Campbell, Mpho Cornelius, South African Heritage Resources Agency, and McGregor Museum. Thank you to UCT staff Louisa Hutton, Dolores Jacobs, Deborah Walbrugh, and Rene van der Merwe, and all student lab and field contributors who helped with this project (Jess von der Meden, Navashni Naidoo, Jani Louw, Leesha Richardson, Nathan Bickerton, Alyssa Eltzholtz, Josh Giesken, Tamara Jeggels, Mabeth Crafford, Tara Edwards, Khumo Matlhoko, Ayanda Mdludlu, Alicen Munn, Chris Shelton, Wendy Khumalo, Patricia Groenwalde, Josie Burness, Michaela Heale, Rachel Westbrook, Trisha Patel, Precious Chaware, Bacara Spruit, Batande Getyengana). Thank you also to the University of Melbourne, John Hellstrom, Petra Bajo, and Helen Green. We are grateful for the constructive comments from Manuel Will and four anonymous reviewers on an earlier version of the manuscript.

Funding Information Funding was provided by the University of Cape Town, National Research Foundation Centre of Excellence (COE) in Palaeosciences, Palaeontological Scientific Trust (PAST), National Research Foundation-African Origins Platform (AOP150924142990), a National Geographic Society-Waitt Grant, and an ARC Discovery Early Career Research Award (DE 190100160).

Compliance with Ethical Standards

Conflict of Interest The authors declare that they have no conflict of interest.

References

- Aitken, M. J. (1985). *Thermoluminescence dating*. London: Academic Press.
- Ambrose, S. H., & Lorenz, K. G. (1990). Social and ecological models for the Middle Stone Age in southern Africa. In P. Mellars (Ed.), *The emergence of modern humans: an archaeological perspective*. Edinburgh: Edinburgh University Press.
- Bader, G. D., Cable, C., Lentfer, C., & Conard, N. J. (2016). Umbeli Belli Rock Shelter, a forgotten piece from the puzzle of the Middle Stone Age in KwaZulu-Natal, South Africa. *Journal of Archaeological Science: Reports*, 9, 608–622.
- Bader, G. D., Tribolo, C., & Conard, N. J. (2018). A return to Umbeli Belli: new insights of recent excavations and implications for the final MSA of eastern South Africa. *Journal of Archaeological Science: Reports*, 21, 733–757.
- Barham, L. S., & Mitchell, P. (2008). *The first Africans: African archaeology from the earliest toolmakers to most recent foragers*. Cambridge: Cambridge University Press.
- Barton, C. M., & Clark, G. A. (1993). Cultural and natural formation processes in late Quaternary cave and rockshelter sites of western Europe and the near east. In Goldberg, P., Nash, D. T., & Petraglia, M. D. (Eds.) *Formation processes in archaeological context*. Madison, Wisc.: Prehistory Press. pp. 33–52.
- Beaumont, P. B., & Morris, D. (1990). *Guide to archaeological sites in the Northern Cape*. Kimberley: McGregor Museum.
- Beaumont, P. B., & Vogel, J. C. (1989). Patterns in the age and context of rock art in the Northern Cape. *The South African Archaeological Bulletin*, 44(150), 73–81.
- Beaumont, P. B., & Vogel, J. C. (2006). On a timescale for the past million years of human history in central South Africa. *South African Journal of Science*, 102, 6–6.
- Benn, D. (1994). Fabric shape and the interpretation of sedimentary fabric data. *Journal of Sedimentary Research*, 64(4a), 910–915.
- Berna, F., Goldberg, P., Kolska Horwitz, L., Brink, J., Holt, S., Bamford, M., & Chazan, M. (2012). Microstratigraphic evidence of in situ fire in the Acheulean strata of Wonderwerk Cave, Northern Cape province, South Africa. *Proceedings of the National Academy of Sciences*, 109(20), E1215–E1220.
- Bernatchez, J. A. (2010). Taphonomic implications of orientation of plotted finds from Pinnacle Point 13B (Mossel Bay, Western Cape Province, South Africa). *Journal of Human Evolution*, 59(3–4), 274–288.
- Binford, L. R. (1982). The archaeology of place. *Journal of Anthropological Archaeology*, 1(1), 5–31.
- Bird, M. I., Ayliffe, L. K., Fifield, L. K., Turney, C. S. M., Cresswell, R. G., Barrows, T. T., & David, B. (1999). Radiocarbon dating of “old” charcoal using a wet oxidation, stepped-combustion procedure. *Radiocarbon*, 41(2), 127–140.
- Botter-Jensen, L., & Mejdahl, V. (1988). Assessment of beta dose-rate using a GM multicounter system. *Nuclear Tracks and Radiation Measurements*, 14(1–2), 187–191.
- Botter-Jensen, L., Andersen, C. E., Duller, G. A. T., & Murray, A. S. (2003). Developments in radiation, stimulation and observation facilities in luminescence measurements. *Radiation Measurements*, 37(4), 535–541.
- Bousman, C. B., & Cruz-Uribe, K. (1998). Strategies for coping with risk: Later Stone Age hunter-gatherers at Blydefontein rock shelter. *Journal of Anthropological Archaeology*, 24.3(2005), 193–226.
- Brain, C. K. (1981). *The hunters or the hunted? An introduction to African cave taphonomy*. Chicago: University of Chicago Press.
- Brooks, A. S., Hare, P. E., Kokis, J. E., Miller, G. H., Ernst, R. D., & Wendorf, F. (1990). Dating Pleistocene archeological sites by protein diagenesis in ostrich eggshell. *Science*, 248(4951), 60–64.

- Brown, K. S., Marean, C. W., Herries, A. I. R., Jacobs, Z., Tribolo, C., Braun, D., Roberts, D. L., Meyer, M. C., & Bernatchez, J. (2009). Fire as an engineering tool of early modern humans. *Science*, 325(5942), 859–862.
- Chazan, M., Porat, N., Sumner, T. A., & Kolska Horwitz, L. (2013). The use of OSL dating in unstructured sands: the archaeology and chronology of the Hutton Sands at Canteen Kopje (Northern Cape Province, South Africa). *Archaeological and Anthropological Sciences*, 5(4), 351–363.
- Chazan, M., Kolska Horwitz, L., Ecker, M., Koopowitz, C., Rhodes, S. E., Morris, D., & Berna, F. (2017). Renewed excavations at Wonderwerk Cave, South Africa. *Evolutionary Anthropology: Issues, News, and Reviews*, 26(6), 258–260.
- Cohen, T. J., Jansen, J. D., Gliganic, L. A., Larsen, J. R., Nanson, G. C., May, J.-H., Jones, B. G., & Price, D. M. (2015). Hydrological transformation coincided with megafaunal extinction in central Australia. *Geology*, 43, 195–198.
- Deacon, H. J. (1976). *Where hunters gathered: a study of Holocene Stone Age people in the eastern Cape* (Vol. 1). Claremont: South African Archaeological Society Monograph Series.
- Deacon, J. (1978). Changing patterns in the Late Pleistocene/Early Holocene prehistory of southern Africa as seen from the Nelson Bay Cave stone artifact sequence. *Quaternary Research*, 10, 84–111.
- Dibble, H. L., Chase, P. G., McPherron, S. P., & Tuffreau, A. (1997). Testing the reality of a “living floor” with archaeological data. *American Antiquity*, 62(4), 629–651.
- Dibble, H., McPherron, S. P., Chase, P., Farrand, W. R., & Debenath, A. (2006). Taphonomy and the concept of Paleolithic cultures: the case of the Tayacian from Fontéchevade. *PaleoAnthropology*, 2006, 1–21.
- Douka, K., Slon, V., Jacobs, Z., Ramsey, C. B., Shunkov, M. V., Derevianko, A. P., Mafessoni, F., Kozlikin, M. B., Li, B., Grün, R., & Comeskey, D. (2019). Age estimates for hominin fossils and the onset of the Upper Palaeolithic at Denisova Cave. *Nature*, 565(7741), 640.
- Ecker, M., Brink, J., Chazan, M., Kolska Horwitz, L., & Lee-Thorp, J. A. (2017). Radiocarbon dates constrain the timing of environmental and cultural shifts in the Holocene strata of Wonderwerk Cave, South Africa. *Radiocarbon*, 59(4), 1067–1086.
- Foley, R. A., & Lahr, M. M. (1997). Mode 3 technologies and the evolution of modern humans. *Cambridge Archaeological Journal*, 7, 3–36.
- Forssman, T. R., et al. (2010). A Later Stone Age assemblage from Canteen Kopje, Northern Cape. *The South African Archaeological Bulletin*, 65(192), 204–214.
- Galbraith, R. (2003). A simple homogeneity test for estimates of dose obtained using OSL. *Ancient TL*, 21, 75–77.
- Galbraith, R. F., Roberts, R. G., Laslett, G. M., Yoshida, H., & Olley, J. M. (1999). Optical dating of single and multiple grains of quartz from Jinmium rock shelter, northern Australia: part I, experimental design and statistical methods. *Archaeometry*, 41, 339–364.
- Gandin, A., Wright, D. T., & Melezhiik, V. (2005). Vanished evaporites and carbonate formation in the Nearchaean Kogelbeen and Gamohaam formations of the Campbellrand subgroup, South Africa. *Journal of African Earth Sciences*, 41(1–2), 1–23.
- Gliganic, L. A., May, J.-H., & Cohen, T. J. (2015). All mixed up: using single-grain equivalent dose distributions to identify phases of pedogenic mixing on a dryland alluvial fan. *Quaternary International*, 362, 23–33.
- Gliganic, L. A., Cohen, T. J., Meyer, M., & Molenaar, A. (2017). Variations in luminescence properties of quartz and feldspar from modern fluvial sediments in three rivers. *Quaternary Geochronology*, 41, 70–82.
- Grün, R., Brink, J. S., Spooner, N. S., Taylor, L., Stringer, C., Franciscus, R. G., & Murray, A. (1996). Direct dating of Florisbad hominid. *Nature*, 382, 500–501.
- Guérin, G., Mercier, N., & Adamiec, G. (2011). Dose-rate conversion factors: update. *Ancient TL*, 29(1), 5–8.
- Hammer, Ø., Harper, D. A. T., & Ryan, P. D. (2001). PAST: paleontological statistics software package for education and data analysis. *Palaeontologia Electronica*, 4(1), 9.
- Hellstrom, J. (2003). Rapid and accurate U/Th dating using parallel ion-counting multi-collector ICP-MS. *Journal of Analytical Atomic Spectrometry*, 18(11), 1346–1351.
- Hellstrom, J. (2006). U–Th dating of speleothems with high initial ²³⁰Th using stratigraphical constraint. *Quaternary Geochronology*, 1(4), 289–295.
- Henshilwood, C. S., d’Errico, F., Vanhaeren, M., Van Niekerk, K., & Jacobs, Z. (2004). Middle Stone Age shell beads from South Africa. *Science*, 304(5669), 404–404.
- Henshilwood, C. S., d’Errico, F., & Watts, I. (2009). Engraved ochres from the Middle Stone Age levels at Blombos Cave, South Africa. *Journal of Human Evolution*, 57(1), 27–47.
- Henshilwood, C. S., d’Errico, F., van Niekerk, K. L., Coquinot, Y., Jacobs, Z., Lauritzen, S.-E., Menu, M., & García-Moreno, R. (2011). A 100,000-year-old ochre-processing workshop at Blombos Cave, South Africa. *Science*, 334(6053), 219–222.

- Henshilwood, C. S., d'Errico, F., van Niekerk, K. L., Dayet, L., Queffelec, A., & Pollarolo, L. (2018). An abstract drawing from the 73,000-year-old levels at Blombos Cave, South Africa. *Nature*, *562*(7725), 115–118.
- Herries, A. I. R. (2011). A chronological perspective on the Acheulian and its transition to the Middle Stone Age in southern Africa: the question of the Fauresmith. *International Journal of Evolutionary Biology*, *2011*, 1–25.
- Hogg, A. G., Hua, Q., Blackwell, P. G., Niu, M., Buck, C. E., Guilderson, T. P., Heaton, T. J., Palmer, J. G., Reimer, P. J., & Reimer, R. W. (2013). SHCal13 Southern Hemisphere calibration, 0–50,000 years cal BP. *Radiocarbon*, *55*(4), 1889–1903.
- Horwitz, L. K., & Chazan, M. (2015). Past and present at Wonderwerk Cave (Northern Cape Province, South Africa). *African Archaeological Review*, *32*(4), 595–612.
- Humphreys, A. J. B. (1974). A preliminary report on test excavations at Dikbosch Shelter I, Herbert District, Northern Cape. *The South African Archaeological Bulletin*, *29*(115/116), 115–119.
- Humphreys, A. J. B., & Thackeray, A. I. (1983). In A. J. B. Humphreys & A. I. Thackeray (Eds.), *Ghaap and Gariiep: Later Stone Age studies in the Northern Cape*. Cape Town: The South African Archaeological Society.
- Huntley, D. J., Godfrey-Smith, D. I., & Thewalt, M. L. W. (1985). Optical dating of sediments. *Nature*, *313*(5998), 105–107.
- Jacobs, Z., Wintle, A. G., Duller, G. A. T., Roberts, R. G., & Wadley, L. (2008). New ages for the post-Howiesons Poort, late and final Middle Stone Age at Sibudu, South Africa. *Journal of Archaeological Science*, *35*, 1790–1807.
- Kaplan, J. (1990). The Umhlatuzana rock shelter sequence: 100,000 years of stone age history. Natal Museum. *Journal of Humanities*, *2*, 1–94.
- Kuman, K., Inbar, M., & Clarke, R. J. (1999). Palaeoenvironments and cultural sequence of the Florisbad Middle Stone Age hominid site, South Africa. *Journal of Archaeological Science*, *26*(12), 1409–1425.
- Lenoble, A., & Bertran, P. (2004). Fabric of Palaeolithic levels: methods and implications for site formation processes. *Journal of Archaeological Science*, *31*(4), 457–469.
- Lotter, M. G., Gibbon, R. J., Kuman, K., Leader, G. M., Forssman, T., & Granger, D. E. (2016). A geoarchaeological study of the Middle and Upper Pleistocene levels at Canteen Kopje, Northern Cape Province, South Africa. *Geoarchaeology*, *31*(4), 304–323.
- Low, M., & Mackay, A. (2016). The Late Pleistocene microlithic at Putslaagte 8 Rockshelter in the Western Cape, South Africa. *South African Archaeological Bulletin*, *71*(204), 146.
- Lukich, V., Porat, N., Faershtein, G., Cowling, S., & Chazan, M. (2019). New chronology and stratigraphy for Kathu Pan 6, South Africa. *Journal of Paleolithic Archaeology*, *2*(3), 235–257.
- Maape, S. 2016. Architecture for resilience: dialogues with place in the indigenous communities of Kuruman during the Holocene period. Dissertation, faculty of engineering and the built environment, University of the Witwatersrand, Johannesburg.
- Mackay, A., Stewart, B. A., & Chase, B. M. (2014). Coalescence and fragmentation in the late Pleistocene archaeology of southernmost Africa. *Journal of Human Evolution*, *72*, 26–51.
- Maggs, T. (1995). Neglected rock art: the rock engravings of agriculturist communities in South Africa. *The South African Archaeological Bulletin*, *50*(162), 132–142.
- Marean, C. W. (2010). Pinnacle Point Cave 13B (Western Cape Province, South Africa) in context: the Cape Floral kingdom, shellfish, and modern human origins. *Journal of Human Evolution*, *59*(3–4), 425–443.
- Marean, C. W. (2014). The origins and significance of coastal resource use in Africa and Western Eurasia. *Journal of Human Evolution*, *77*, 17–40.
- Marean, C. W. (2015). An evolutionary anthropological perspective on modern human origins. *Annual Review of Anthropology*, *44*, 533–556.
- Marean, C. W. (2016). The transition to foraging for dense and predictable resources and its impact on the evolution of modern humans. *Philosophical Transactions of the Royal Society B: Biological Sciences*, *371*(1698), 20150239.
- Marean, C. W., Nilssen, P. J., Brown, K., Jerardino, A., & Stynder, D. (2004). Paleoanthropological investigations of Middle Stone Age sites at Pinnacle Point, Mossel Bay (South Africa): archaeology and hominid remains from the 2000 field season. *Paleoanthropology*, *2*, 14–83.
- Marean, C. W., Bar-Matthews, M., Bernatchez, J., Fisher, E., Goldberg, P., Herries, A. I. R., Jacobs, Z., Jerardino, A., Karkanas, P., Minichillo, T., Nilssen, P. J., Thompson, E., Watts, I., & Williams, H. M. (2007). Early human use of marine resources and pigment in South Africa during the Middle Pleistocene. *Nature*, *449*(7164), 905–908.
- McBrearty, S., & Brooks, A. S. (2000). The revolution that wasn't: a new interpretation of the origin of modern human behavior. *Journal of Human Evolution*, *39*(5), 453–563.

- McPherron, S. J. P. (2005). Artifact orientations and site formation processes from total station proveniences. *Journal of Archaeological Science*, 32(7), 1003–1014.
- McPherron, S. P. (2018). Additional statistical and graphical methods for analyzing site formation processes using artifact orientations. *PLoS One*, 13(1), e0190195.
- Mellars, P. (2006). Why did modern human populations disperse from Africa ca. 60,000 years ago? A new model. *Proceedings of the National Academy of Sciences*, 103(25), 9381–9386.
- Morris, D. (1988). Engraved in place and time: a review of variability in the rock art of the Northern Cape and Karoo. *The South African Archaeological Bulletin*, 43(148), 109–120.
- Morris, D., & Beaumont, P. B. (2004). *Archaeology in the Northern Cape: some key sites*. Kimberley: McGregor Museum.
- Morris, D., Pinto, L., & Louw, J. (2018). A dolomite rock gong at Ga-Mohana, a ritual site in the Kuruman Hills. *The Digging Stick*, 35(2), 7–8.
- Murray, A. S., & Wintle, A. G. (2000). Luminescence dating of quartz using an improved single-aliquot regenerative-dose protocol. *Radiation measurements*, 32(1), 57–73.
- Oestmo, S., Schoville, B. J., Wilkins, J., & Marean, C. W. (2014). A Middle Stone Age Paleoscape near the Pinnacle Point caves, Vleesbaai, South Africa. *Quaternary International*, 350, 147–168.
- Palmison, M. E. 2014. Excavation, analysis, and intersite comparison of the Robberg industry components at the open-air site of Erfkroon, South Africa. Thesis, Anthropology Department, Texas State University.
- Pargeter, J., & Redondo, M. (2016). Contextual approaches to studying unretouched bladelets: A late Pleistocene case study at Sehonghong Rockshelter, Lesotho. *Quaternary International*, 404, 30–43.
- Parkington, J. (2010). Coastal diet, encephalization, and innovative behaviors in the late Middle Stone Age of southern Africa. *Human brain evolution: The influence of freshwater and marine food resources*, 189–202.
- Porat, N., Chazan, M., Grün, R., Aubert, M., Eisenmann, V., & Kolska Horwitz, L. (2010). New radiometric ages for the Fauresmith industry from Kathu Pan, southern Africa: implications for the Earlier to Middle Stone Age transition. *Journal of Archaeological Science*, 37(2), 269–283.
- Porraz, G., Parkington, J. E., Rigaud, J.-P., Miller, C. E., Poggenpoel, C., Tribolo, C., Archer, W., Cartwright, C. R., Charrié-Duhaut, A., Dayet, L., Igreja, M., Mercier, N., Schmidt, P., Verna, C., & Texier, P.-J. (2013). The MSA sequence of Diepkloof and the history of southern African Late Pleistocene populations. *Journal of Archaeological Science*, 40(9), 3542–3552.
- Prescott, J. R., & Hutton, J. T. (1994). Cosmic ray contributions to dose rates for luminescence and ESR dating: large depths and long-term time variations. *Radiation Measurements*, 23, 497–500.
- Rhodes, E. J. (2011). Optically stimulated luminescence dating of sediments over the past 200,000 years. *Annual Review of Earth and Planetary Sciences*, 39, 461–488.
- Robbins, L. H., Murphy, M. L., Brook, G. A., Ivester, A. H., Campbell, A. C., Klein, R. G., et al. (2000). Archaeology, palaeoenvironment, and chronology of the Tsodilo Hills White Paintings Rock Shelter, northwest Kalahari desert, Botswana. *Journal of Archaeological Science*, 27, 1085–1113.
- Roberts, R. G., Galbraith, R. F., Yoshida, H., Laslett, G. M., & Olley, J. M. (2000). Distinguishing dose populations in sediment mixtures: a test of single-grain optical dating procedures using mixtures of laboratory-dosed quartz. *Radiation Measurements*, 32, 459–465.
- Schiffer, M. B. (1987). *Formation processes of the archaeological record*. Albuquerque: University of New Mexico.
- Smith, E. I., Jacobs, Z., Johnsen, R., Ren, M., Fisher, E. C., Oestmo, S., Wilkins, J., Harris, J. A., Karkanas, P., Fitch, S., Ciravolo, A., Keenan, D., Cleghorn, N., Lane, C. S., Matthews, T., & Marean, C. W. (2018). Humans thrived in South Africa through the Toba eruption about 74,000 years ago. *Nature*, 555(7697), 511.
- Soriano, S., Villa, P., & Wadley, L. (2007). Blade technology and tool forms in the Middle Stone Age of South Africa: the Howiesons Poort and post-Howiesons Poort at Rose Cottage Cave. *Journal of Archaeological Science*, 34(5), 681–703.
- Sumner, D. Y. (1997). Carbonate precipitation and oxygen stratification in late Archean seawater as deduced from facies and stratigraphy of the Gamohaam and Frisco formations, Transvaal Supergroup, South Africa. *American Journal of Science*, 297(5), 455–487.
- Sumner, D. Y., & Bowring, S. A. (1996). U-Pb geochronologic constraints on deposition of the Campbellrand subgroup, Transvaal Supergroup, South Africa. *Precambrian Research*, 79(1), 25–35.
- Texier, P.-J., Porraz, G., Parkington, J., Rigaud, J.-P., Poggenpoel, C., Miller, C., Tribolo, C., Cartwright, C., Coudenneau, A., Klein, R., Steele, T., & Verna, C. (2010). A Howiesons Poort tradition of engraving ostrich eggshell containers dated to 60,000 years ago at Diepkloof Rock Shelter, South Africa. *Proceedings of the National Academy of Sciences*, 107(14), 6180–6185.

- Thackeray, F., & Thackeray, A. I. (1980). *Report on a preliminary survey of archaeological sites in the central Northern Cape Province* (pp. 1–29). National Monuments Council Permit PER/1/231.
- Thomsen, K. J., Murray, A., & Jain, M. (2012). The dose dependency of the over-dispersion of quartz OSL single grain dose distributions. *Radiation Measurements*, 47(9), 732–739.
- Tooth, S., Hancox, P. J., Brandt, D., McCarthy, T. S., Jacobs, Z., & Woodborne, S. (2013). Controls on the genesis, sedimentary architecture, and preservation potential of dryland alluvial successions in stable continental interiors: insights from the incising Modder River, South Africa. *Journal of Sedimentary Research*, 83(7), 541–561.
- Van der Merwe, N. J., Sealy, J., & Yates, R. (1987). First accelerator carbon-14 date for pigment from a rock painting. *South African Journal of Science*, 83(1), 56–57.
- Villa, P., Delagnes, A., & Wadley, L. (2005). A late Middle Stone Age artifact assemblage from Sibudu (KwaZulu-Natal): comparisons with the European Middle Paleolithic. *Journal of Archaeological Science*, 32, 399–422.
- Wadley, L. (2005). A typological study of the final Middle Stone Age stone tools from Sibudu Cave, KwaZulu-Natal. *South African Archaeological Bulletin*, 60, 51–63.
- Wadley, L. (2015). Those marvellous millennia: the Middle Stone Age of southern Africa. *Azania: Archaeological Research in Africa*, 50(2), 155–226.
- Wadley, L., Sievers, C., Bamford, M., Goldberg, P., Berna, F., & Miller, C. (2011). Middle Stone Age bedding construction and settlement patterns at Sibudu, South Africa. *Science*, 334(6061), 1388–1391.
- Wasson, K., Woolfolk, A., & Fresquez, C. (2013). Ecotones as indicators of changing environmental conditions: rapid migration of salt marsh–upland boundaries. *Estuaries and Coasts*, 36(3), 654–664.
- Watts, L., Chazan, M., & Wilkins, J. (2016). Early evidence for brilliant ritualized display: specularite use in the Northern Cape (South Africa) between ~500 ka and ~300 ka. *Current Anthropology*, 57, 287–309.
- Wilkins, J. (2017). Middle Pleistocene lithic raw material foraging strategies at Kathu Pan 1, Northern Cape, South Africa. *Journal of Archaeological Science: Reports*, 11, 169–188.
- Wilkins, J., & Chazan, M. (2012). Blade production ~500 thousand years ago at Kathu Pan 1, South Africa: support for a multiple origins hypothesis for early Middle Pleistocene blade technologies. *Journal of Archaeological Science*, 39(6), 1883–1900.
- Wilkins, J., Schoville, B. J., Brown, K. S., & Chazan, M. (2012). Evidence for early hafted hunting technology. *Science*, 338, 942–946.
- Will, M., Kandel, A. W., & Conard, N. J. (2019). Midden or molehill: the role of coastal adaptations in human evolution and dispersal. *Journal of World Prehistory*, 32(1), 33–72.
- Wurz, S., Evjenth Bentsen, S., Reynard, J., Van Pletzen-Vos, L., Brenner, M., Mentzer, S., Pickering, R., & Green, H. (2018). Connections, culture and environments around 100 000 years ago at Klasies River main site. *Quaternary International*, 495, 102–115.
- Ziegler, M., Simon, M. H., Hall, I. R., Barker, S., Stringer, C., & Zahn, R. (2013). Development of Middle Stone Age innovation linked to rapid climate change. *Nature Communications*, 4, 1905.

Publisher's Note Springer Nature remains neutral with regard to jurisdictional claims in published maps and institutional affiliations.

Affiliations

Jayne Wilkins^{1,2,3} · Benjamin J. Schoville^{2,3,4} · Kyle S. Brown^{2,3} · Luke Gliganic⁵ · Michael C. Meyer⁵ · Emma Loftus^{3,6} · Robyn Pickering^{3,7} · Benjamin Collins^{2,3,8} · Alexander F. Blackwood^{3,9} · Simangaliso Makalima^{2,3} · Amy Hatton^{3,10} · Sechaba Maape¹¹

¹ Australian Research Centre for Human Evolution, Environmental Futures Research Institute, Griffith University, 170 Kessels Road, Nathan, Brisbane, QLD 4111, Australia

² Department of Archaeology, University of Cape Town, Private Bag X3, Rondebosch, Cape Town 7701, South Africa

³ Human Evolution Research Institute, University of Cape Town, Private Bag X3, Rondebosch, Cape Town 7701, South Africa

⁴ School of Social Science, University of Queensland, St. Lucia, Queensland 4072, Australia

- ⁵ Department of Geology, University of Innsbruck, Innrain 52, 6020 Innsbruck, Austria
- ⁶ McDonald Institute for Archaeological Research, University of Cambridge, Downing Street, Cambridge CB2 3ER, UK
- ⁷ Department of Geological Sciences, University of Cape Town, Private Bag X3, Rondebosch, Cape Town 7701, South Africa
- ⁸ Department of Anthropology, University of Manitoba, 15 Chancellor Circle, Winnipeg, Manitoba R3T 2N2, Canada
- ⁹ Department of Archaeology and History, La Trobe University, Bundoora, Melbourne, Victoria 3068, Australia
- ¹⁰ Institute of Archaeology, University College London, 31-34 Gordon Square, London WC1H 0PY, UK
- ¹¹ School of Architecture and Planning, University of the Witwatersrand, Yale Rd, Johannesburg 2000, South Africa